COMPUTATIONAL CONTINUUM MECHANICS

ВЫЧИСЛИТЕЛЬНАЯ МЕХАНИКА СЛОШНЫХ СРЕД

Computational Continuum Mechanics. 2021. Vol. 14. No. 3. pp. 333-348 DOI: 10.7242/1999-6691/2021.14.3.28

CRITERION FOR ELASTOPLASTIC FRACTURE OF A BIMETALLIC PLATE WITH AN EDGE TRANSVERSE SHEAR CRACK AT THE MATERIAL INTERFACE

V.D. Kurguzov[1,2] and N.V. Fedorova[1,3]

[1]*Lavrentyev Institute of Hydrodynamics SB RAS, Novosibirsk, Russian Federation*
[2]*Novosibirsk State University, Novosibirsk, Russian Federation*
[3]*Novosibirsk State Technical University, Novosibirsk, Russian Federation*

The initiation of an edge transverse shear crack in elastoplastic materials that fail under ultimate strain is considered. The crack propagation criterion is formulated using a modified Leonov – Panasyuk – Dugdale model which includes an additional parameter — the width of the plasticity zone. The coupled quasi-brittle fracture criterion for mode II cracks in an elastoplastic material is specified for small-scale yield conditions in the presence of a singularity of the stress field in the vicinity of the crack tip. The coupled fracture criterion includes the strain criterion, which is used at the crack tip, as well as the stress criterion, which is applied at the model crack tip. The lengths of the initial and model cracks differ by the length of the pre-fracture zone. The sequential analysis of the possibility of applying the proposed fracture criterion in determining the critical loads for solids containing edge transverse shear cracks at the interface of different media is performed. Quasi-brittle fracture diagrams are constructed for a composite plate with an edge crack under plane strain and plane stress conditions. The analysis of the parameters included in the proposed model of quasi-brittle fracture is carried out. The model parameters are proposed to be selected by approximation of simple shear diagram and critical stress intensity factor. The critical loads were found numerically for the quasi-ductile and ductile fracture types. The finite element method is used to solve the problem of drawing out a reinforcing layer from a metal composite under quasi-static loading. The process of propagation of plastic zones in the vicinity of the crack tip is described consistently. It is shown that the shapes of the constructed plastic zones differ significantly from the well-known classical concepts.

Key words: brittle, quasi-brittle, quasi- ductile and ductile fracture; elastoplastic materials, limiting strain

1. Introduction

The inevitable formation of cracks is one of the most important factors causing the destruction of engineering structures. The most common crack-like defects are located in places of stress concentration, as a rule in the vicinity of the tips of cuts, at the boundaries of holes, and in composite materials along the interface between media. Therefore, the problems of formulation simple, suitable for engineering calculations, analytical models of the fracture process of materials and structures are relevant.

The advantages and disadvantages of stress and strain fracture criteria are discussed in [1–5], and all reasoning is carried out only on the basis of one-parameter local fracture criteria for brittle and quasi-brittle materials. However, another view of the fracture process is possible, when it occurs according to a non-classical fracture scheme, in which, in addition to its two classical states of the material (solid and fractured), a third, intermediate state is taken into account. This state corresponds to pre-fracture, taking into account damage accumulation in the vicinity of stress concentrators. The use of multiparameter fracture criteria suggests itself when considering a nonclassical fracture scheme [6–11]. The state of a mechanically stressed material is between brittle and ductile, the difference between which, in the mechanical aspect, is determined by the ratio of energy costs for reversible and irreversible deformation phenomena. In this regard, there is a need to assess the state of the material according to two criteria with a continuous transition from one to another. The implementation of the two-parameter fracture criterion makes it possible to combine the areas of applicability of one-parameter fracture criteria that correspond to different limit states of the material. Such a criterion can be based on one-parameter criteria: force, deformation, energy, and their combinations [12–19]. In [20–22], a two-parameter (coupled) integral fracture criterion in an elastoplastic material was proposed and fracture diagrams were constructed for flat specimens in the presence of sharp internal cracks of normal separation (fracture mode I). A simple representation of the pre-fracture zone in the

Email addresses for correspondence: kurguzov@hydro.nsc.ru

form of a rectangle was obtained on the basis of the modified Leonov–Panasyuk–Dugdale model [23, 24] and the Neuber–Novozhilov approach for materials with a structure [25, 26]. Critical curves are plotted under the conditions of necessity and sufficiency of fracture criteria on the "crack length–stress" plane, dividing this plane into three subdomains. These areas correspond to the absence of fracture, the accumulation of damage in the pre-fracture zone, and the separation of the specimen into parts. The selection of fracture diagrams constant in the analytical description of quasi-brittle materials in the presence of cracks is carried out using the approximation of the classical "stress-strain" diagram of the initial material and the critical stress intensity factor (SIF). It should be noted that the dual fracture criterion proposed by Leguilon [3] is suitable only for brittle fracture.

In this article, the couple fracture criterion is used to determine critical loads for the mode II edge crack in a plate made of an elastoplastic material. The proposed approach is based on the notion that the nucleation and growth of cracks, regardless of temperature, are preceded by the following processes: elastic deformation of the material, transition to the plastic state, development of plastic deformations, exhaustion of the plasticity resource, and fracture. Cold brittleness, which is a consequence of a decrease in the plasticity of the material, is determined from static tests. In a number of materials at low temperatures, in addition to reducing plasticity, a crack is able to pass through the grain, which also reduces the fracture toughness of the material.

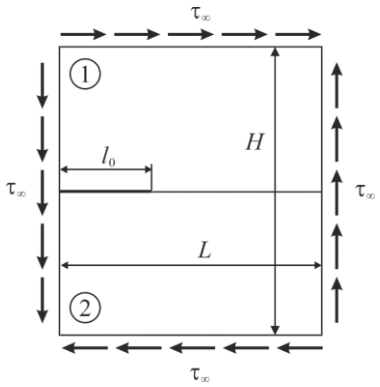

Fig. 1. Scheme of loading the bimetallic plate with the edge crack along the material interface.

The proposed model uses a non-classical scheme of material failure, when, along with the continuous and destroyed states, some intermediate state of the material with accumulated damage is considered. The results obtained in this work make it possible to evaluate the bearing capacity of structures with cracks in a wider range of loading conditions than it is possible with one-parameter criteria of fracture mechanics.

2. Formulation of the problem

The most common crack-like defects are located in composites along the interface. Therefore, the study of the stress-strain state in the problem of the transverse shear crack propagation in a composite is of interest. A composite piecewise homogeneous bimetal plate is considered. The plate width is L; the plate height is H; the edge crack of length l_0 is located on the flat interface of two materials 1 and 2 (Fig.1). The surface of the crack is free from loads, τ_∞ is the shear stress at the edges of the plate. The fracture mode II is realized. The materials of the plate are considered to be elastic – perfectly plastic: G_1, G_2 are the shear moduli; ν_1, ν_2 are the Poisson's ratios; τ_{Y1} τ_{Y2} are the yield strengths under simple shear.

Let us assume that a flat transverse shear crack propagates in a straight line. In addition to a real length crack-cut l_0, a model crack-cut is introduced into consideration, the length of which is $l = l_0 + b$, where b is the prefracture zone length on continuation of the real crack. The fracture problem has two linear scales: if the average grain diameter d is determined by the structure of the material, then the second linear scale is generated by the system itself. This second linear scale is the length of the pre-fracture zone b, which changes in accordance with: 1) the length of the real crack and 2) the intensity of loading change. It should be noted that the critical length of the pre-fracture zone b^* – is a well-defined parameter for a single loading of quasi-brittle materials ($l^* = l_0 + b^*$ – critical macrocrack length).

The $(\tau - \gamma)$ strain diagram is obtained when testing the specimen under shear (Fig. 2), where τ is the shear stress; γ is the shear strain. Let us take the simplest approximation of the real $(\tau - \gamma)$-diagram of the material under study, when this diagram is approximated by a two-link polyline. With a bi-linear approximation of the initial material diagram, the material is replaced by an elastic – perfectly plastic material, with an ultimate strain, upon reaching which the material is destroyed. Fig.

2 shows the original $(\tau-\gamma)$ - diagram (curve *1*) and its two-link approximation (curve *2*). The parameters of this approximation are chosen so that the areas under curves *1* and *2* coincide. The curve *2* is determined by the parameters: G is the shear modulus; τ_Y is the shear yield strength; γ_0 is the maximum elastic strain; γ_1 is the maximum strain. The yield strength and maximum elastic strain are related by the relation: $\tau_Y = G\gamma_0$. The approximation of the $(\tau-\gamma)$ - diagrams at the section $\gamma_0 < \gamma < \gamma_1$ can be interpreted as a perfect plasticity, and the ratio $(\gamma_1-\gamma_0)/\gamma_0$ as the ductility of the material under a monotonic shear.

It is assumed that the region of nonlinear effects is small compared to the crack length in quasi-brittle fracture. This allows us to consider that the size of this region and the intensity of plastic deformations in it are entirely controlled by the stress intensity factor K_{II} and the yield strength τ_Y. This region is so small that the stress field around it is still described by the asymptotic formulas [27]. The type of material failure can be classified according to the relative size of the pre-fracture zone as follows: $b=0$ – brittle, $b/l_0 \ll 1$ – quasi-brittle, $b/l_0 \approx 1$ – quasi-viscous, $b/l_0 \geq 1$ – viscous [20-22].

3. The Leonov - Panasyuk – Dugdale fracture model

Assume that materials *1* and *2* of the upper and lower halves differ only in different shear yield strengths $\tau_Y = \tau_{Y1} < \tau_{Y2}$, i. e. the case of an "almost" homogeneous plate is considered. The stress-strain state near the crack tip is investigated, and a model is constructed to describe the delamination of the composite, assuming that the crack does not change its initially straight direction during propagation. Let d be the characteristic linear size of the material structure (average grain diameter) [22]. The Neiber–Novozhilov approach [25, 26] makes it possible to use solutions for media with a structure that have a singular component with an integrable singularity.

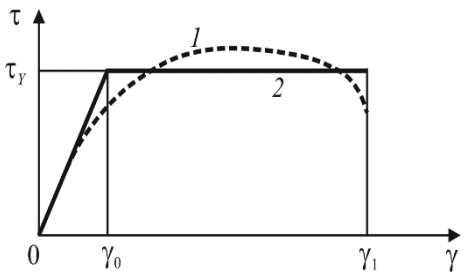

Fig. 2. The original $(\tau-\gamma)$ - diagram (curve 1) and its bi-linear approximation (curve 2).

When constructing diagrams of quasi-brittle fracture, sufficient fracture criteria are used [20–22] in a wide range of crack lengths. The sufficient coupled fracture criterion can be represented by two relations for short macrocracks and medium microcracks:

$$\frac{1}{d}\int_0^d \tau_{xy}(x)dx = \tau_Y\,, \tag{1}$$

$$2u(-b^*) = \delta^*. \tag{2}$$

Here, $\tau_{xy}(x)$ – shear stresses on the continuation of a model crack in a rectangular coordinate system Oxy, moreover, the origin of coordinates coincides with the tip of the model crack in the modified Leonov – Panasyuk – Dugdale model [23, 24], and the axis Ox is directed along the crack (Fig. 3, *a*); $2u = 2u(x)$ is the total transverse displacement (displacement difference of the corresponding points) of the model crack faces ($x<0$); δ^* – is the critical transverse displacement of the crack edges for a homogeneous material (in this displacement, the structure of the material at the tip of a real crack is destroyed due to the shear); b^* is the critical length of the pre-fracture zone. According to V.V. Novozhilov' terminology [26], criterion (1) is necessary, since it controls the beginning of the fracture process and the set of conditions (1), (2) is a sufficient criterion for fracture; the critical values obtained according to the sufficient and necessary fracture criteria are marked with the upper symbols * and ^{0} respectively. The necessity of criterion (1) lies in the fact that it controls the beginning of the destruction process, and the set of criteria (1), (2) is sufficient, since when both

conditions are met, the final fracture of the specimen occurs. It should be noted that the proposed criterion (1), (2) is dual: the formulation of the strain fracture criterion (2) refers to the tip of the original crack, and the stress criterion (1) for shear stresses, taking into account averaging, to the tip of the model crack.

Figure 3 shows shear stresses $\tau_{xy} = -\tau_Y$, acting on the crack extension according to the Leonov–Panasyuk–Dugdale model, and an approximation of the plastic zone (conventionally depicted as an ellipse) in the form of a rectangular pre-fracture zone with sides a and b homogeneous ($\tau_{Y1} = \tau_{Y2}$) material (Fig. 3b). Stresses $\tau_{xy} = -\tau_Y$, on the edges of the model crack in the pre-fracture zone, opposite in sign to the stresses $\tau_{xy} = \tau_\infty$ on the plate faces, prevent the crack from opening in the transverse direction. The pre-fracture zone occupies only a part of the plastic zone.

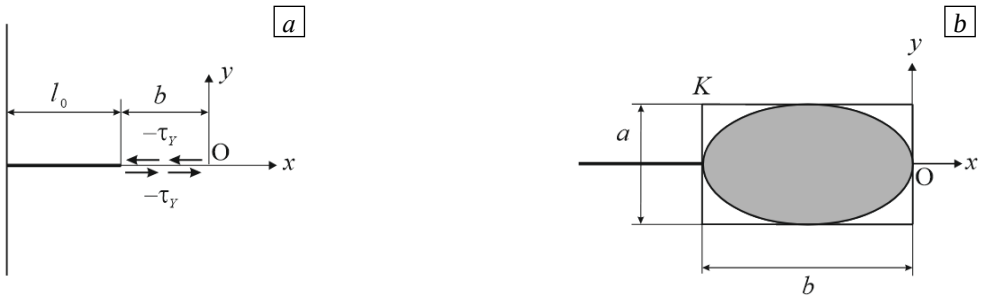

Fig. 3. Shear stresses acting, according to the Leonov–Panasyuk–Dugdale model, on the extension of a crack (a); approximation of the plastic zone in the form of a rectangular pre-fracture zone of a homogeneous material (b).

4. Diagrams of quasi-brittle fracture of a biomaterial

Shear stress field $\tau_{xy}(x)$ on the extension of a model crack $x > 0$ can be represented as the sum of two terms [28]:

$$\tau_{xy}(x) = \frac{K_{\text{II}}}{\sqrt{2\pi x}} + \tau_{nom}. \tag{3}$$

where $\tau_{nom} = Y_r \tau_\infty$ — nominal stresses, otherwise, estimation of the regular part of the stress field in the vicinity of the model crack tip; $Y_r = Y_r(l/L)$ is the correction factor that takes into account the width of the plate L, $l = l_0 + b$; $K_{\text{II}} = K_{\text{II}\infty} + K_{\text{II}b} > 0$ is the total stress intensity factor, where $K_{\text{II}\infty} > 0$ s the stress intensity factor generated by specified test conditions, $K_{\text{II}b} < 0$ is the stress intensity factor generated by constant stresses $-\tau_Y$, acting in the pre-fracture zone. For definiteness, the stresses τ_∞ and τ_{nom} are considered positive, and the stresses $-\tau_Y$, acting in the pre-fracture zone are negative. The terms in relation (3) are the singular and regular parts of the solution, respectively. In the dual criterion, equality (1) controls the process of reaching the yield strength τ_Y by averaged stresses, and equality (2) describes the transverse shear at the tip of a real macrocrack.

Estimate singular components of stress fields for edge cracks. Since the deformation of materials is measured under conditions of small-scale yield, specimens with edge cracks for the initial SIF have ideas [29]:

$$K_{\text{II}\infty} = Y_s \tau_\infty \sqrt{\pi l}, \qquad Y_s = \sqrt{\frac{2L}{\pi l} \operatorname{tg} \frac{\pi l}{2L}}, \qquad K_{\text{II}b} = -\tau_Y \sqrt{\pi l}\, \frac{2}{\pi} \arccos\left(1 - \frac{b}{l}\right). \tag{4}$$

When considering quasi-brittle fracture under low-scale yield conditions, taking into account the approximation:

$$\frac{b}{l} \approx 1, \tag{5}$$

up to values of the highest order of smallness for the multiplier $\arccos\left(1-b/l\right)$ in relation (4) the expression is true: $\arccos\left(1-b/l\right) \approx \sqrt{2b/l}$. The final simplified notation $K_{\text{II}b}$ will be as follows:

$$K_{\text{II}b} = -2\tau_Y \sqrt{\frac{2b}{\pi}}. \tag{6}$$

The correction factor $Y_r = Y_r\left(l/L\right)$ is taken in the form: $Y_r = L/\left(L-l\right)$, which corresponds to the approximation of the strength of material. As $l \to L$, then $\tau_{nom} \to \infty$. That shows an increase in stresses when the net cross section decreases to zero at a constant load. For an edge crack of a transverse shear in a half-plane $Y_s = Y_r = 1$.

Under the conditions of small-scale yield (5), in the presence of a singular component in the solution and the rejection of secondary terms, the displacement of the model crack edges can be represented as [28]:

$$u\left(x\right) = \frac{\kappa+1}{4G} K_{\text{II}} \sqrt{\frac{-2x}{\pi}}, \quad x \le 0, \tag{7}$$

where $G = \tau_Y/\gamma_0$ is the shear modulus of a homogeneous material, κ is the stress state parameter ($\kappa = 3-4\nu$ for plane strain, $\kappa = \left(3-\nu\right)/\left(1+\nu\right)$ for plane stress).

The critical displacement of the model crack edges δ^* in relation (2) depends on the plasticity margin of the material under study ($\gamma_1 - \gamma_0$, see Fig. 2) and the width of the prefracture zone at the tip of the real crack:

$$\delta^* = m\left(\gamma_1 - \gamma_0\right) a, \tag{8}$$

where m is the correction factor. Assume that in the case of a localized plastic flow, the width of the prefracture zone a in relation (8) is proportional to the diameter of the plastic zone for a transverse shear crack in ideally plastic bodies. In an approximate formulation, the shape and dimensions of the plastic zone in the vicinity of the tip of a transverse shear crack in a homogeneous material for plane deformation using the von Mises yield criterion are determined by the relation [30]:

$$r_p\left(\theta\right) = \frac{K_{\text{II}\infty}^2}{4\pi\sigma_Y^2}\left[\frac{3}{2} + \frac{9}{2}\cos^2\theta + \left(1-2\nu\right)^2\left(1-\cos\theta\right)\right]. \tag{9}$$

where r_p is the radius of the plastic zone; θ is the polar angle; $\sigma_Y = \sqrt{3}\tau_Y$ is the uniaxial strained yield strength. For a plane stress state, the shape of the plastic zone can be easily determined from (9), assuming $\nu = 0$. Figure 4 shows the boundaries of plastic zones, plotted in dimensionless variables $4\pi\sigma_Y^2 r_p\left(\theta\right)/K_{\text{II}\infty}^2$, in the vicinity of the tip of the transverse shear crack for a homogeneous material

($\tau_{Y1} = \tau_{Y2}$) and a bimaterial. It is assumed that at $\tau_{Y1} < \tau_{Y2}$ the plastic zone is exactly equal to half of the plastic zone of a homogeneous material.

Assuming in (9) $\theta = \pi/2$ for a homogeneous material under plane deformation, we obtain:

$$a = 2r_p\left(\frac{\pi}{2}\right) = \frac{K_{\text{II}\infty}^2}{4\pi\sigma_Y^2}\left[3+2(1-2\nu)^2\right] = \frac{K_{\text{II}\infty}^2}{12\pi\tau_Y^2}\left[3+2(1-2\nu)^2\right] = \frac{\chi}{\pi}\left(\frac{K_{\text{II}\infty}}{\tau_Y}\right)^2, \qquad (10)$$

where $\chi = \left[3+2(1-2\nu)^2\right]/12$. For a one-sided plasticity zone, the value a in (10) should be reduced by half. The plane stress state follows from (10) at $\nu = 0$. The critical shear of the model crack edges δ^* in relation (8) is chosen so that the material at the tip of a real crack is destroyed in the case when the limiting deformation of the material γ_1 is reached.

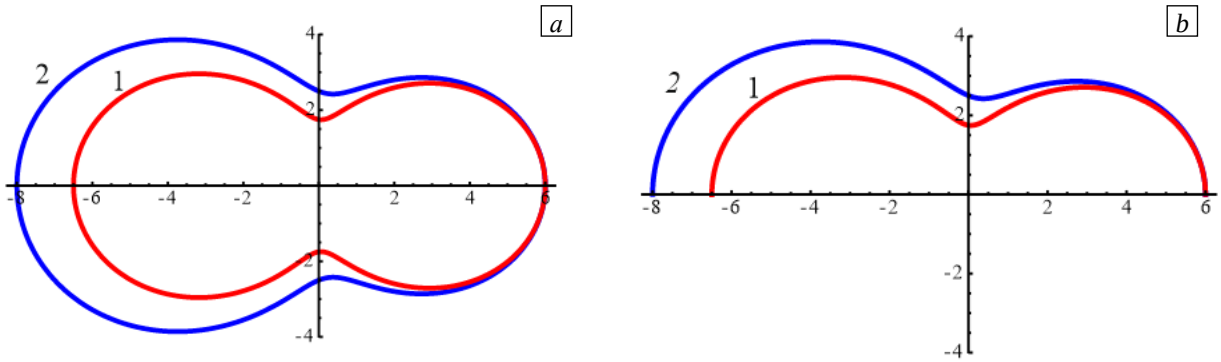

Fig. 4. The boundaries of plastic zones (according to the Mises criterion) in the vicinity of the tip of a transverse shear crack in a homogeneous material (*a*) and a one-sided plasticity zone in a bimaterial (*б*); plane deformation at $\nu = 0,25$ (curve 1, plane stress state (2).

Estimate the critical state of the material at the crack tip. Relations (3), (4), (6)–(8), (10) contain all the necessary analytical expressions for applying the sufficient (double) criterion (1), (2). By integrating in (1), we find:

$$K_{\text{II}} = \left(\tau_Y - Y_r\tau_\infty^*\right)\sqrt{\frac{\pi d}{2}}. \qquad (11)$$

Substituting (7), (8), (10) into (2), we obtain:

$$\frac{\kappa+1}{2G}K_{\text{II}}\sqrt{\frac{2b^*}{\pi}} = m\left(\gamma_1-\gamma_0\right)\frac{\chi}{\pi}\left(\frac{K_{\text{II}\infty}}{\tau_Y}\right)^2. \qquad (12)$$

Transform (11) using relations (4) for the SIF $K_{\text{II}} = K_{\text{II}\infty} + K_{\text{II}b}$:

$$Y_s\bar{\tau}_\infty^*\sqrt{\frac{2l^*}{d}} - \frac{2}{\pi}\sqrt{\frac{2l^*}{d}}\sqrt{\frac{2b^*}{l^*}} = 1 - Y_r\bar{\tau}_\infty^*. \qquad (13)$$

Here $\bar{\tau}_\infty^* = \tau_\infty^*/\tau_Y$ is the dimensionless critical stresses in the plate. Taking into account that $G = \tau_Y/\gamma_0$, from (12):

$$\left(Y_s\bar{\tau}_\infty^* - \frac{2}{\pi}\sqrt{\frac{2b^*}{l^*}}\right)\sqrt{\frac{2b^*}{l^*}} = \frac{2m\chi}{\kappa+1}\bar{\gamma}_{\text{II}}\left(Y_s\bar{\tau}_\infty^*\right)^2, \tag{14}$$

where $\bar{\gamma}_{\text{II}} = \left(\gamma_1 - \gamma_0\right)/\gamma_0$ is the parameter characterizing the margin of plasticity in shear. After opening the brackets on the left side of equation (14), the factor b^*/l^*, appears, which, due to inequality (5), can be discarded as a value of a higher order of smallness compared to $\sqrt{b^*/l^*}$. As a result, the system of equations (13), (14) will contain terms with the factor $\sqrt{b^*/l^*}$.

Solving the system of equations, (13), (14), we find analytical expressions for the dimensionless critical length of the pre-fracture zone $\bar{b}^* = b^*/l^*$ and dimensionless critical load $\bar{\tau}_\infty^* = \tau_\infty^*/\tau_Y$:

$$\bar{b}^* = 2\left(\frac{m\chi}{\kappa+1}\bar{\gamma}_{\text{II}}Y_s\bar{\tau}_\infty^*\right)^2, \tag{15}$$

$$\bar{\tau}_\infty^* = \left[Y_r + \left(1 - \frac{4m\chi}{\pi(\kappa+1)}\bar{\gamma}_{\text{II}}\right)Y_s\sqrt{2\bar{l}^*}\right]^{-1}, \tag{16}$$

where $\bar{l}^* = l^*/d$ is the dimensionless critical crack length. It follows from the condition of the ultimate load limited $\bar{\tau}_\infty^* \le 1$ that in (16) the expression in parentheses must be positive. As a result, we obtain a limit on the plasticity margin of the material:

$$\bar{\gamma}_{\text{II}} < \frac{\pi\left(\kappa+1\right)}{4m\chi} = \gamma_m. \tag{17}$$

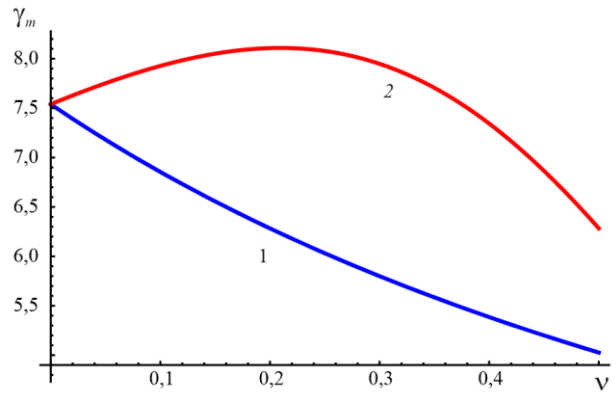

Fig. 5. Dependence γ_m (see (17)) on Poisson's ratio ν in the case of a plane stress state (curve 1), for plane strain (2).

Inequality (17) is the constraint under which quasi-brittle fracture occurs under conditions of small-scale yield of a homogeneous material in the pre-fracture zone. Figure 5 shows the dependence γ_m on the Poisson's ratio for the plane stress state (curve 1) and plane strain (curve 2) at the value of the correction factor $m = 1$. As can be seen from the presented plots, curve 1 passes below curve 2 for any $0 < \nu \le 0{,}5$. Taking into account the range of parameters κ and χ, we find that for any ν under plane deformation and plane stress state, the inequality $\bar{\gamma}_{\text{II}} \le 5{,}027$ should be satisfied.

In the limit at $\gamma_1 \to \gamma_0$ relation (16) implies an expression corresponding to the required failure criterion:

$$\bar{\tau}_\infty^0 = \left(Y_r + Y_s\sqrt{2\bar{l}_0}\right)^{-1}. \tag{18}$$

Here $\bar{\tau}_\infty^0 = \tau_\infty^0 / \tau_Y$ is the dimensionless critical load; $\bar{l}_0 = l_0 / d$ is the dimensionless length of the initial crack. Relation (18) describes the brittle fracture of materials. It is obvious that $\bar{\tau}_\infty^0 < \bar{\tau}_\infty^*$ at $l_0 < l^*$.

The effective diameter of the fracture structure d for sufficiently long cracks is found from the formula [12]:

$$d = \frac{2}{\pi}\left(\frac{K_{\text{IIc}}}{\tau_Y}\right)^2, \tag{19}$$

where K_{IIc} is the critical SIF at destruction in II mode. If the critical SIF K_{IIc} and the classical $(\tau - \gamma)$-diagram (more precisely, its approximation) were obtained in two laboratory experiments, by using three parameters $d, \tau_Y, \bar{\gamma}_{\text{II}}$, in a wide range of crack lengths, two critical curves can be plotted: $\bar{\tau}_\infty^0 = \bar{\tau}_\infty^0\left(\bar{l}_0, \bar{L}\right)$, $\bar{\tau}_\infty^* = \bar{\tau}_\infty^*\left(\bar{l}^*, \bar{L}\right)$, which depend on the crack lengths $\bar{l}_0$, $\bar{l}^*$ and the dimensionless plate width $\bar{L} = L/d$.

Let us combine compatible plane $\left(\bar{l}_0, \bar{\tau}_\infty^0\right)$ and $\left(\bar{l}^*, \bar{\tau}_\infty^*\right)$, and in the "crack length–stress" coordinates $\left(\bar{l}, \bar{\tau}_\infty\right)$, where $\bar{l} = l/d$, $\bar{\tau}_\infty = \tau_\infty / \tau_Y$, we plot diagrams of quasi-brittle fracture for a bimetallic plate (hereinafter referred to as the specimen). Let the loading intensity be given $\bar{\tau}_\infty$. Then the diagram of quasi-brittle fracture makes it possible to estimate the state of the body with a crack. Two critical curves $\bar{\tau}_\infty^0$ and $\bar{\tau}_\infty^*$ divide the plane $\left(\bar{l}, \bar{\tau}_\infty\right)$ into three parts: a subregion $\bar{\tau}_\infty < \bar{\tau}_\infty^0$, where there are no damages; subdomain $\bar{\tau}_\infty^0 < \bar{\tau}_\infty < \bar{\tau}_\infty^*$, where damage accumulation in the pre-fracture zone takes place in the material; subdomain $\bar{\tau}_\infty > \bar{\tau}_\infty^*$, where failure occurs under monotonic loading.

Figure 6 shows the dimensionless critical stresses $\bar{\tau}_\infty^0 = \bar{\tau}_\infty^0\left(\bar{l}_0, \bar{L}\right)$ (curves 1–5) and $\bar{\tau}_\infty^* = \bar{\tau}_\infty^*\left(\bar{l}^*, \bar{L}, \bar{\gamma}_{\text{II}}\right)$ (curves 1'–5') of samples with an edge crack in double logarithmic coordinates. For a specific implementation of the calculations, the following parameters were chosen: $\bar{L} = 200, 400, 800, 1600, \infty$ for pairs of curves *1–1'*, *2–2'*, *3–3'*, *4–4'*, *5–5'*, respectively, and $4m\chi\bar{\gamma}_{\text{II}}/\left(\pi\left(\kappa+1\right)\right) = 0,6$. Pairs of curves *1–1'*, *2–2'*, *3–3'*, *4–4'*, *5–5'* represent quasi-brittle fracture diagrams for the considered type of specimens made from a homogeneous material.

Thus, formulas have been obtained for calculating the critical breaking load (16) and, through it, the critical length of the pre-fracture zone (see 15). These expressions are suitable for both homogeneous and "almost" homogeneous samples, when materials 1 and 2 of the upper and lower halves of the plate differ only in shear yield strength $\tau_{Y1} < \tau_{Y2}$, and the shear moduli, Poisson's ratios and the characteristic linear dimensions of the material structures are the same. It is assumed that only one of the weakest components is in such a bimaterial under plasticity conditions, and the width of the pre-fracture zone characteristic of it in the bimaterial is approximately chosen as the width of the pre-fracture zone. In this case, in formulas (15)–(17) one should put $\chi = \left[3 + 2\left(1-2\nu\right)^2\right]/24$.

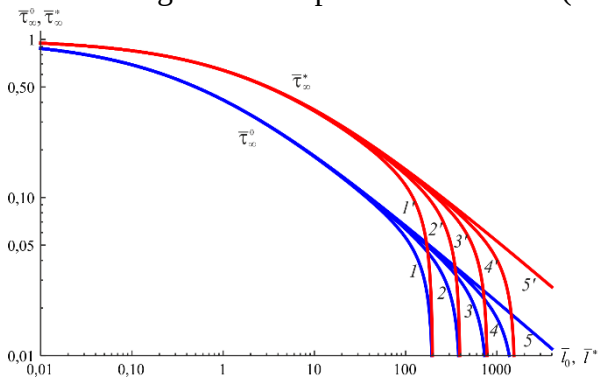

Fig.6. Quasi-brittle fracture diagrams.

Let us consider an edge crack at the connection line of two dissimilar materials with elastic constants G_1, ν_1 (upper half), G_2, ν_2 (lower half) и and shear yield strengths $\tau_{Y1} < \tau_{Y2}$. Then, under the action of both pure tension (I mode) and pure shear (II mode), tangential and normal stresses (I + II mode) will appear on the continuation of the crack in a solid body. As a result, when implementing the failure criterion for dissimilar materials, it is necessary to take into account both stress intensity factors K_{I} and K_{II}, in contrast to a homogeneous medium [31–34]. The expressions for the stress components obtained in [34] are a good approximation for describing the behavior of a composite body, with the exception of the regions located near the crack tips. However, the expressions for the coefficients K_{I} and K_{II} proposed in [33] include the logarithm of the crack length, so when they are substituted into the corresponding equations above, the results will be unphysical.

From a practical point of view, such a parameter as the rate of release of elastic energy, which is identical to the Rice–Cherepanov integral [35, 36] seems to be more suitable when calculating the strength of structures under conditions of elastoplastic deformation. J-integral is often used as a failure parameter [37]. The expression for the J-integral in terms of stress intensity factors has the following form [38]:

$$J = \frac{1}{16}\left[\frac{1+\kappa_1}{G_1} + \frac{1+\kappa_2}{G_2}\right] K\overline{K}, \tag{20}$$

where $K = K_{\text{I}} - iK_{\text{II}}$ is complex stress intensity factor, the bar above indicates the complex conjugate value. In [39] the concept of the equivalent stress intensity factor: $K_e = \sqrt{K\overline{K}}$, was introduced, with the help of which it was found that in a wide range of changes in the G_1/G_2 K_e differs from K_{II} by less than 4.5% for plane strain, and less than 5.1% for a plane stress state. Therefore, in the case of substantially heterogeneous materials, it can be considered fulfilled with the error of up to 5% of the ratio, (15)–(18), which is quite acceptable from an engineering point of view. For calculations, you should choose the characteristics of the material with a lower yield strength.

5. Computer simulation

An approximate statement of the problem of localized plastic flow is formulated in linear fracture mechanics and implies that the solution in the elastic region is described only by the main terms of the asymptotic expansion in the vicinity of the crack tip (3), the solution in the plastic zone is not considered at all, and the boundary of localized plastic flow (9) is determined based on the elastic stress field and the selected yield criterion. Since here we are not talking about any attempt at elastoplastic analysis, it is clear that the results obtained are far from reality and cannot give reliable estimates of the shape and size of the plastic zone [20].

Let us use the finite element method for numerical simulation of the real shape of the plastic zone propagating along the interface between two materials. Consider a plate with the width of $L = 25$ mm (axis Ox), the length of $H = 50$ mm with a flat edge crack of the length $l_0 = 5$ mm. The plate is deformed under simple shear conditions under the action of shear stress τ_∞, applied to the edges H and faces L of the plate in opposite directions, as shown in Figure 7. Plane deformation conditions are assumed to be satisfied. The edge crack is located at the same distance from the short faces, and its front is parallel to the axis Ox. The kinematic boundary conditions on the faces H with coordinates $y = 0$ and $y = 50$ are given as $\upsilon = 0$, and at the crack tip with coordinates $y = 25$, $x = 5$ the boundary conditions are $u = \upsilon = 0$ for a homogeneous plate (shown in Fig. 7) and $u = 0$, if it is bimetallic.

The problem was solved in two versions: a) the plate material was considered homogeneous with Young's modulus $E = 200$ GPa, Poisson's ratio $\nu = 0,25$, yield strength in uniaxial tension $\sigma_Y = 400$

MPa and, therefore, shear yield strength $\tau_Y = \sigma_Y / \sqrt{3} = 230{,}94$ MPa, the applied load was equal to $\tau_\infty = 200$ MPa; b) a bimetallic plate with a crack at the interface, the elastic characteristics of the materials were the same, only the yield strengths differed: $\sigma_{Y1} = 200$ MPa, $\sigma_{Y2} = 400$ MPa, the load $\tau_\infty = 100$ MPa acted.

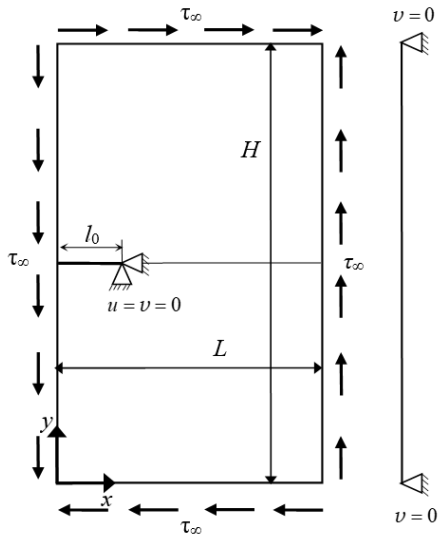

Fig. 7. Scheme of fixing and loading of the plate with a simple shear.

The computational domain was uniformly divided into 80,000 nodal rectangular elements with a quadratic approximation of displacements. The mesh of finite elements was thickened to the axis of the crack in order to most accurately determine the shape and dimensions of the plastic zone. Near the axis of the crack, the elements had a size (side length) of 0.1 mm. During loading, the external load increased monotonically from zero to τ_∞ by 100 time steps. At loading levels $\bar{\tau} = \tau_\infty / \tau_Y > 0{,}5$ in the vicinity of the crack tip, large plastic deformations occurred, so the problem was solved on the basis of the general equations of mechanics of a deformable solid body in the current Lagrangian formulation, taking into account the physical and geometric nonlinearity [40]. The stress-strain state was calculated using the MSC.Marc 2018 finite element analysis package [41] with the "largestrain" option. The calculated plastic zones in a homogeneous plate under plane deformation are shown in Figure 8.

The distribution of equivalent plastic strains $\varepsilon^p = \sqrt{2\varepsilon_{ij}^p \varepsilon_{ij}^p / 3}$ (ε_{ij}^p are components of the plastic strain tensor) at different levels of loading is given.

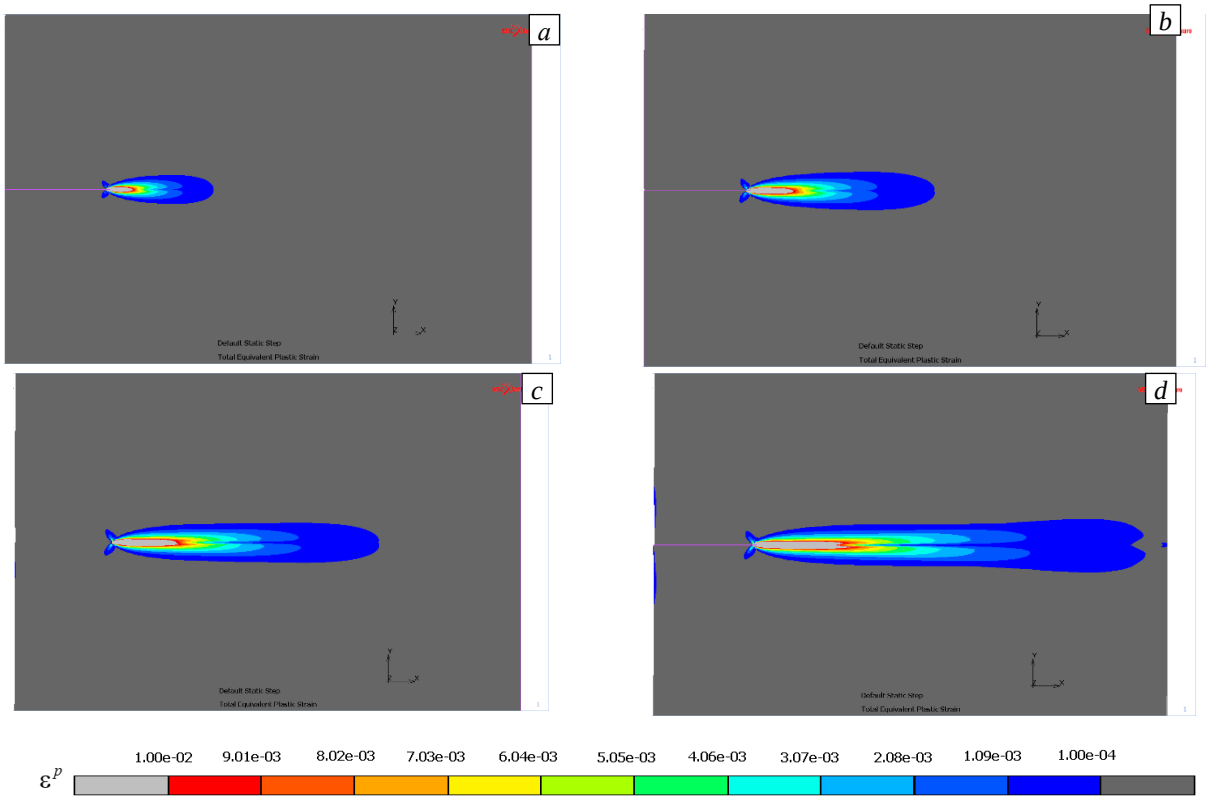

Fig.8. Shapes of plastic zones in a homogeneous plate under plane deformation conditions at different acting loads $\bar{\tau}$: 0,76 (*a*); 0,86 (b); 0,91 (c); 0,93 (d) ε^p.

Figure 9 shows the distribution of equivalent plastic deformations in a bimetallic plate under plane deformation conditions at different loading levels $\overline{\tau}$.

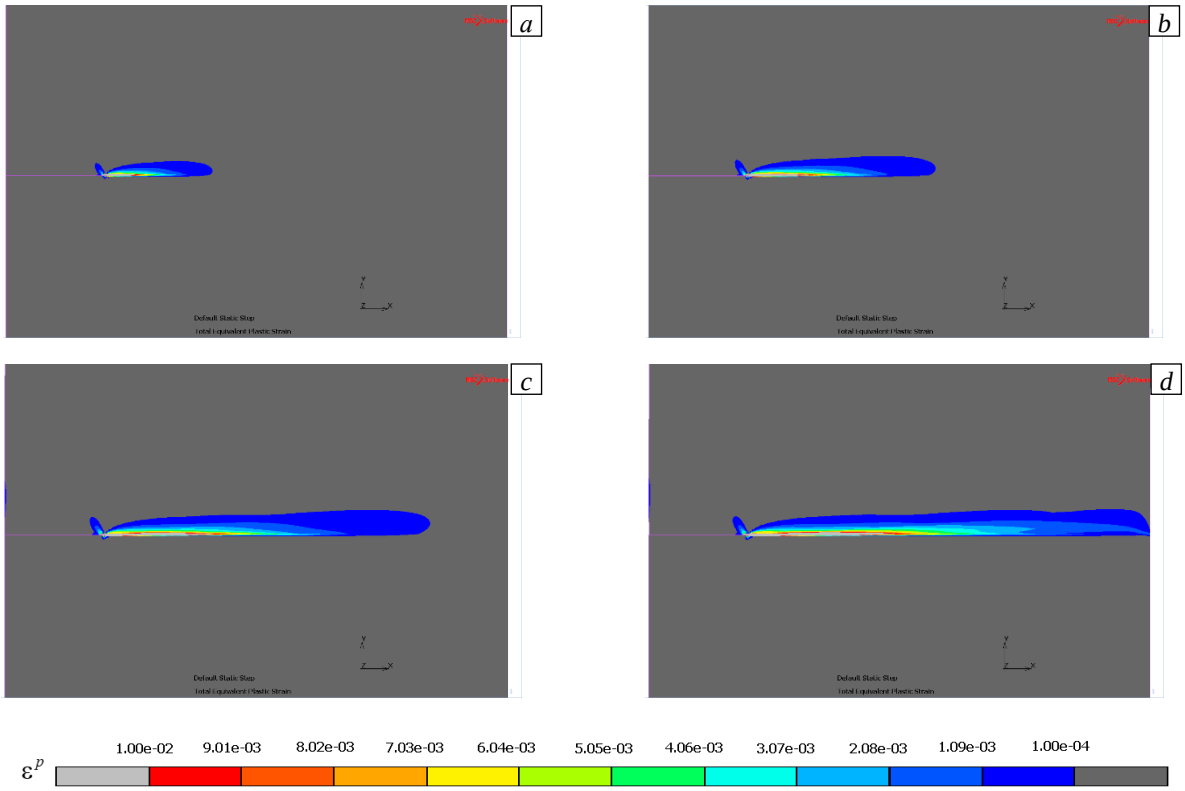

Fig. 9. Forms of plastic zones in a bimetallic plate under plane deformation and different levels of loading $\overline{\tau}$: 0,785 (*a*), 0,885 (b), 0,938 (c), 0,94 (d).

The contour lines in figures 8, 9 are limited by the range of values $10^{-4} \div 10^{-2}$ for a more detailed drawing of the distribution of equivalent plastic strain ε^p . The crack is located to the left of the plastic zone, the region of plastic deformations exceeding 0.01 is located directly in front of the crack tip. The plastic zone stretches in the direction of the crack axis and becomes flatter as the load increases. The plastic zone increases with a further increase in the load and at $\overline{\tau} = 0,94$ reaches the right edge of the plate.

The table shows the lengths b and width a of the plastic zone with simple shear under conditions of plane deformation and various loads for a plate made of homogeneous and bimetallic materials, obtained as a result of a numerical solution. The width a was defined as the maximum width of the plastic zone along the crack extension; the length of this zone b is shown in Figure 3b. The results show that the crack width in a bimetallic plate is approximately 2 times smaller than in a plate made of a homogeneous material.

Table. Dimensions of the plastic zone established in numerical calculations for simple shear under plane deformation conditions for plates made of homogeneous and bimetallic material

Homogeneous plate			Bimetal plate		
$\overline{\tau}$	b , mm	a , mm	$\overline{\tau}$	b , mm	a , mm
0,76	4,90	1,43	0,785	5,30	0,72
0,86	8,65	1,81	0,885	9,30	0,97
0,91	13,00	1,95	0,938	16,10	1,04
0,93	18,80	1,95	0,940	20,00	1,04

The results of the numerical calculation reflect the real shape of the plastic zone for a plate made of a homogeneous material in the form of a narrow elongated symmetrical "jug" with a "neck" in the vicinity of the crack tip, and for a bimetallic plate, the plastic zone of a similar shape is one-sided and is located in the area corresponding to the material with a lower limit yield stress. However, they are neither in shape nor in size similar to the plastic zones shown in Figure 4 in the case of the plain strain state for the plate made of a homogeneous bimetallic material. For example, for a homogeneous plate at $\bar{\tau} = 0,91$ from (9), (10) we obtain: $a = 1,249$ mm, $b = 4,273$ mm; numerical calculation gives the values: $a = 1,945$ mm, $b = 13,00$ mm. As can be seen, the length of the plastic zone b is three times greater than the value given by formula (9). In this regard, in [42, 43] to refine the expression for the width of the pre-fracture zone, the insertion of a correction factor m into relation (8) is substantiated. To determine the value of this coefficient, it is necessary to use directly the data of either a numerical or laboratory experiment. Figure 10 shows the dependence of the width of the plastic zone a on the load $\bar{\tau}$. One of them is calculated by formula (10) (curve 1), the other one is plotted according to numerical calculation data. Constraint (5) under conditions of small-scale plastic flow is fulfilled at loads $\bar{\tau} < 0,3$. From a comparison of analytical values with numerical values in this range of loads, we obtain an approximate value of the correction factor $m \approx 2$.

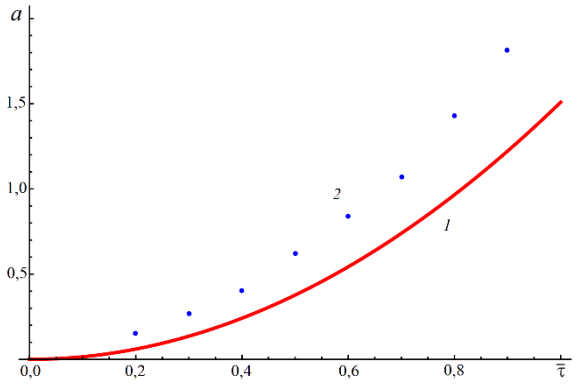

Fig.10. Comparison of the dependence on the load $\bar{\tau}$ of the size of the width of the plastic zone a, obtained by formula (10) (curve 1) and established numerically (2).

6. The problem of extension a reinforcing layer from a metal composite

Let us study the process of delamination of the reinforcement from the matrix when the reinforcement is pulled out of the composite. In [44, 45], when studying the dynamic processes of deep drawing (deepening) of metal composites with discrete fibers under dynamic pulse action on reinforcement, a mathematical model of the motion of a rigid plastic rod in a medium with resistance was realized. Let us consider a similar problem in a quasi-static setting. The scheme of loading a composite plate is shown in Figure 11. The plane strain conditions are assumed to be satisfied. Due to the symmetry of the computational domain (dash-dotted line), its half is modeled. Here: plate length $L = 50$ mm; thickness 10 mm; binder width (aluminum – A) $H = 25$ mm; reinforcement width (steel – S) $h = 5$ mm. There is a section of delamination – an edge crack with a length of $l_0 = 5$ mm. A distributed load is applied to the end of the reinforcing layer (fiber) F. For the "matrix-reinforcement" system, an ideal elastoplastic model with the following characteristics is considered:

– for steel, Young's modulus $E = 200$ GPa, Poisson's ratio $\nu = 0,25$, uniaxial tensile yield strength $\sigma_Y = 400$ MPa;

– for aluminum Young's modulus $E = 70$ GPa, Poisson's ratio $\nu = 0,34$, uniaxial tensile yield strength $\sigma_Y = 100$ MPa.

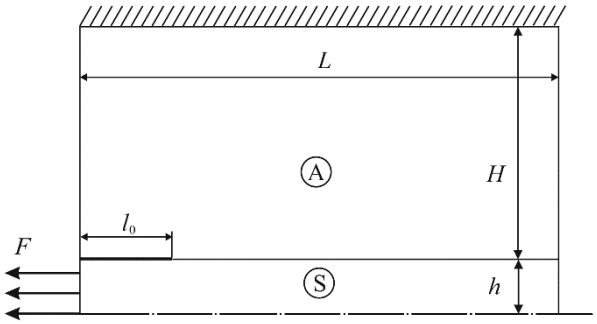

Fig.11. Scheme of fixing and loading of a composite plate.

At the initial moment of stretching of the reinforcing layer, a stress state of simple shear arises – the crack starts in the II mode of destruction, therefore, the critical loads at small-scale yield can be found using formulas (15)–(18), and in the case of the developed plastic flow, the critical load is determined by the finite element method.

The computational domain was covered with a non-uniform mesh of 150,000 nodal rectangular elements with a quadratic approximation of displacements and a complete stress integration scheme. The mesh was refined from the outer boundaries to the crack axis in a ratio of 10:1. During loading, the external load $\sigma_\infty = F/S$, where S — is the cross-sectional area of the reinforcing layer, increased monotonically linearly from zero to $\sigma_Y = 400$ MPa, using an adaptive time step. At loading levels $\bar{\sigma} = \sigma_\infty/\sigma_Y > 0,4$ in the vicinity of the crack tip, large plastic deformations occur; therefore, the problem was solved on the basis of the general equations of mechanics of a deformable solid body in the current Lagrangian formulation, taking into account the physical and geometric nonlinearity [40]. The stress-strain state was calculated using the MSC.Marc 2018 finite element analysis package [41].

The plastic zones plotted according to the calculation data along the interface on the side of the binder are shown in Figure 12. The distribution of equivalent plastic strain ε^p at different levels of loading is given. As before, the contour lines limit the range $10^{-4} \div 10^{-2}$ for their more detailed drawing. The plastic zone stretches in the direction of the crack axis and forms a “hump” as the load increases (Fig. 12d).

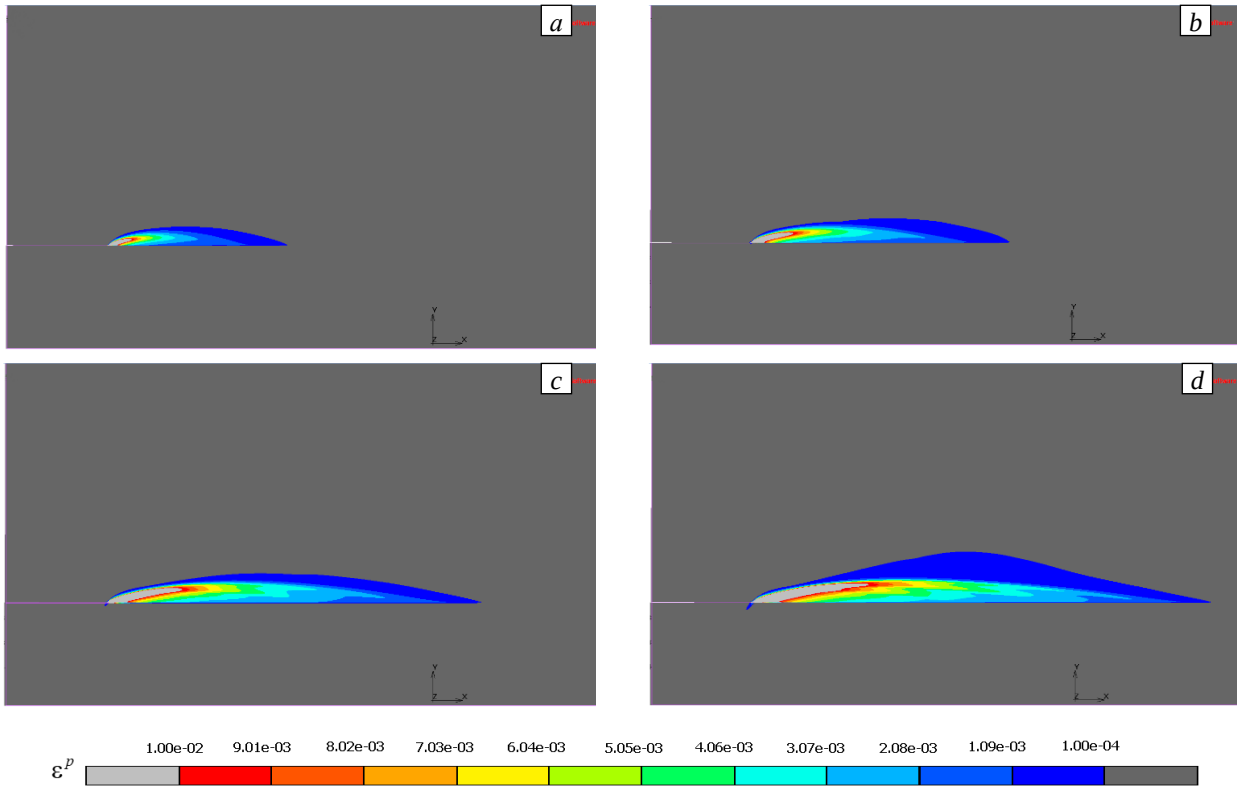

Fig. 12. Forms of plastic zones in the binder at the interface between materials at different levels of external load $\bar{\sigma}$: 0,685 (*a*); 0,785 (*b*); 0,885 (*c*); 0,968 (*d*).

The algorithm for numerically finding the critical load according to the necessary and sufficient criterion was as follows. Some value of the plasticity parameter was set, for example, $\bar{\gamma}_{II} = 40$, which corresponded to 12% plastic strain. At each load step $\bar{\sigma}$ as a result of the analysis of the isolines of the plastic zones, by interpolation over the neighboring nodes of the finite element mesh, the maximum width of the plastic zone $a = a(\bar{\sigma})$ and the transverse displacement $u = u(\bar{\sigma})$ at the point located at a distance $a = a(\bar{\sigma})$ from the crack tip were determined (see point K in Fig. 3b). Further,

according to formula (8), the critical value of the share was calculated $\delta^* = (\gamma_1 - \gamma_0)a = \bar{\gamma}_{II}\gamma_0 a$. There were two successive steps in the load, on one of them, the inequality $u < \delta^*$ was fulfilled, and on the other, the inequality $u > \delta^*$ was fulfilled. By interpolation in time, the load $\bar{\sigma}^*$, was determined at which the transverse displacement u became equal to the critical shear δ^*. The obtained value $\bar{\sigma}^*$ was the critical load according to the sufficient criterion (1), (2).

The critical load according to the required criterion (1) was established at such a time step when the finite elements closest to the crack tip in the interval d completely passed into the plastic state. The numerical calculation showed good agreement with the analytical model at loading levels up to 0.26. A significant discrepancy between the dimensions of the plasticity zone was observed under conditions of full-scale plastic flow, corresponding to the solution of the problem in a geometrically nonlinear formulation in the theory of small deformations.

7. Conclusion

The initiation of a transverse shear crack (fracture mode II) in elastoplastic materials with ultimate strain is considered. The class of materials under study includes, for example, low alloy steels used in structures operating at temperatures below the cold brittleness threshold. The process of destruction of such a material is described in terms of the modified Leonov–Panasyuk–Dugdale model, which uses an additional parameter—the width of the plasticity zone (the width of the pre-fracture zone). A two-parameter quasi-brittle fracture criterion for type II cracks in an elastoplastic material is formulated under small-scale yield conditions in the presence of a singular feature of the stress field in the vicinity of the crack tip, while its deformation part refers to the tip of the original crack, and the force part (written for shear stresses with allowance for averaging) — to the top of the model crack. The lengths of the original and model cracks differ by the length of the pre-fracture zone. A consistent analysis of the applicability of the proposed strength criterion in determining the breaking loads for bodies containing transverse shear cracks is carried out.

Diagrams of quasi-brittle fracture of a plate with an edge transverse shear crack are plotted for the case of monotonic loading. These diagrams consist of two curves dividing the plane in the “crack length–stress” coordinates into three successive subareas, in which, respectively, there are no fractures, damage accumulates in the pre-fracture zone, and the specimen is divided into parts. The analysis of the parameters included in the proposed model of quasi-brittle fracture is carried out, and the conclusion is made about the expediency of their selection according to the $(\tau - \gamma)$–diagram of simple shear and the critical stress intensity factor K_{IIc}.

Expressions are obtained (see 15–18), relating the critical load and the length of the pre-fracture zone. They can be useful for predicting the critical failure load and estimating the length of the pre-fracture zone when loading specimens in mode II in structured materials, since the following quantities are used: d is the characteristic linear size of the material structure; τ_Y and $\bar{\gamma}_{II} = (\gamma_1 - \gamma_0)/\gamma_0$ are the parameters $(\tau - \gamma)$-diagram of simple shear. All three parameters are found as a result of a laboratory experiment. The approximation of the localized plastic flow turns out to be insufficient at such load levels at which plastic zones appear that are comparable with the characteristic dimensions of the problem. The analytical model has a number of limitations that allow its applicability only in the case of small-scale plasticity $b \ll l$ and a small yield plateau length $\bar{\gamma}_{II} \le 5,027$, as follows from (17). The last inequality is satisfied, for example, for heat-resistant steels.

Ultimate loads are found numerically for quasi-viscous and viscous types of fracture. Computer simulation of the propagation of plasticity zones from the tip of a type II crack during the pulling of a reinforcing layer from a metal composite was carried out using the finite element method. An estimate of the dimensions of the plastic zone in the vicinity of the crack tip is obtained. The difference between the numerical model and the analytical one lies in the fact that, on its basis, such materials are studied, the characteristics of which correspond to the deformation regimes at full-scale yield. Large deformations occur in the vicinity of the crack tip, so the problem is solved in the current

Lagrangian formulation, taking into account physical and geometric nonlinearities, based on the general equations of mechanics of a deformable solid body. It has been found that the results of numerical experiments are in good agreement with the results of calculations based on the analytical model of fracture materials with a structure under transverse shear in the small-scale yield regime.

References

1. Berto F, Lazzarin P. Recent developments in brittle and quasi-brittle failure assessment of engineering materials by means of local approaches. *Mater. Sci. Eng. R Rep.*, 2014, vol. 75, pp. 1-48. https://doi.org/10.1016/j.mser.2013.11.001
2. Zhu X.-K., Joyce J.A. Review of fracture toughness (G, K, J, CTOD, CTOA) testing and standardization. *Eng. Fract. Mech.*, 2012, vol. 85, pp. 1-46. https://doi.org/10.1016/j.engfracmech.2012.02.001
3. Leguillon D. Strength or toughness? A criterion for crack onset at a notch. *Eur. J. Mech. Solid.*, 2002, vol. 21, pp. 61-72. https://doi.org/10.1016/S0997-7538(01)01184-6
4. Newman J.C., James M.A., Zerbst U. A review of the CTOA/CTOD fracture criterion. *Eng. Fract. Mech.*, 2003, vol. 70, pp. 371-385. https://doi.org/10.1016/S0013-7944(02)00125-X
5. Weißgraeber P., Leguillon D., Becker W. A review of finite fracture mechanics: crack initiation at singular and non-singular stress raisers. *Arch. Appl. Mech.*, 2016, vol. 86, pp. 375-401. https://doi.org/10.1007/s00419-015-1091-7
6. Zhu X.K., Chao Y.J. Specimen size requirements for two-parameter fracture toughness testing. *Int. J. Fract.*, 2005, vol. 135, pp. 117-136. https://doi.org/10.1007/s10704-005-3946-3
7. Meliani M.H., Matvienko Y.G., Pluvinage G. Two-parameter fracture criterion ($K_{\rho,c}$-$T_{ef,c}$) based on notch fracture mechanics. *Int. J. Fract.*, 2011, vol. 167, pp. 173-182. https://doi.org/10.1007/s10704-010-9542-1
8. Newman Jr. J.C., Newman III J.C. Validation of the Two-Parameter Fracture Criterion using finite-element analyses with the critical CTOA fracture criterion. *Eng. Fract. Mech.*, 2015, vol. 136, pp. 131-141. https://doi.org/10.1016/j.engfracmech.2015.01.021
9. Warren J.M., Lacy T., Newman Jr. J.C. Validation of the Two-Parameter Fracture Criterion using 3D finite-element analyses with the critical CTOA fracture criterion. *Eng. Fract. Mech.*, 2016, vol. 151, pp. 130-137. https://doi.org/10.1016/j.engfracmech.2015.11.007
10. *Matvienko Y.G.* Two-parameter fracture mechanics in contemporary strength problems. *J. Mach. Manuf. Reliab.*, 2013, vol. 42, pp. 374-381. https://doi.org/10.3103/S1052618813050087
11. Matvienko Yu.G., Nikishkov G.P. Two-parameter J-A concept in connection with crack-tip constraint. *Theor. Appl. Fract. Mech.*, 2017, vol. 92, pp. 306-317. https://doi.org/10.1016/j.tafmec.2017.04.007
12. Nikishkov G.P., Matvienko Yu.G. Elastic-plastic constraint parameter a for test specimens with thickness variation. *Fatigue Fract. Engng. Mater. Struct.*, 2016, vol. 39, pp. 939-949. https://doi.org/10.1111/ffe.12390
13. Matvienko Y.G., Morozov E.M. Two basic approaches in a search of the crack propagation angle. *Fatigue Fract. Engng. Mater. Struct.*, 2017, vol. 40, pp. 1191-1200. https://doi.org/10.1111/ffe.12583
14. Popova N.S., Morozov E.M., Matvienko Y.G. Predicting the crack path in a wedge under a concentrated tensile force by means of variational principle. *Frattura ed Integrità Strutturale*, 2019, vol. 13, pp. 267-271. https://doi.org/10.3221/IGF-ESIS.49.26
15. Guo W. Three-dimensional analyses of plastic constraint for through-thickness cracked bodies. *Eng. Fract. Mech.*, 1999, vol. 62, pp. 383-407. https://doi.org/10.1016/S0013-7944(98)00102-7
16. Wang X. Elastic T-stress for cracks in test specimens subjected to non-uniform stress distributions. *Eng. Fract. Mech.*, 2002, vol. 69, pp. 1339-1352. https://doi.org/10.1016/S0013-7944(01)00149-7
17. Wang X., Lewis T., Bell R. Estimations of the T-stress for small cracks at notches. *Eng. Fract. Mech.*, 2006, vol. 73, pp. 366-375. https://doi.org/10.1016/j.engfracmech.2005.06.009
18. Nazarali Q., Wang X. The effect of T -stress on crack-tip plastic zones under mixed-mode loading conditions. *Fatigue Fract. Engng. Mater. Struct.*, 2011, vol. 34, pp. 792-803. https://doi.org/10.1111/j.1460-2695.2011.01573.x
19. Cicero S., Madrazo V., Carrascal I.A. Analysis of notch effect in PMMA using the theory of critical distances. *Eng. Fract. Mech.*, 2012, vol. 86, pp. 56-72. https://doi.org/10.1016/j.engfracmech.2012.02.015
20. Kornev V.M. Estimation diagram of quasi-brittle fracture for bodies with a hierarchy of structures. Multiscale necessary and sufficient fracture criteria. *Fiz. mezomekh. – Physical Mesomechanics*, 2010, vol. 13, no. 1, pp. 47-59.
21. Kornev V.M., Demeshkin A.G. Quasi-brittle fracture diagram of structured bodies in the presence of edge cracks. *J. Appl. Mech. Tech. Phy.*, 2011, vol. 52, pp. 975-985. https://doi.org/10.1134/S0021894411060162

22. Kornev V.M. Critical fracture curves and effective structure diameter of brittle and quasi-brittle materials. *Fiz. mezomekh. – Physical Mesomechanics*, 2013, vol. 16, no. 5, pp. 25-34.
23. Leonov M.Ya., Panasyuk V.V. Razvitiye mel'chayshikh treshchin v tverdom tele [Small cracks growth in a solids]. *Prikladnaya mekhanika – International Applied Mechanics*, 1959, vol. 5, no. 4, pp. 391-401.
24. Dugdale D.S. Yielding of steel sheets containing slits. *J. Mech. Phys. Solid.*, 1960, vol. 8, pp. 100-104. https://doi.org/10.1016/0022-5096(60)90013-2
25. Neuber G. *Kerbspannunglehre: Grunglagen fur GenaueSpannungsrechnung* [Notch Stress Theory: Basics for Exact Stress Calculation]. Springer-Verlag, 1937. 160 p.
26. Novozhilov V.V. On a necessary and sufficient criterion for brittle strength. *J. Appl. Math. Mech.*, 1969, vol. 33, pp. 201-210. https://doi.org/10.1016/0021-8928(69)90025-2
27. Anderson T.L. *Fracture mechanics: Fundamentals and applications*. CRC Press, 2005. 680 p.
28. Gross D., Seelig T. *Fracture mechanics*. Springer, 2006. 320 p.
29. Savruk M.P. *Mekhanika razrusheniya i prochnost' materialov. T. 2. Koeffitsiyenty intensivnosti napryazheniy v telakh s treshchinami* [Fracture mechanics and strength of materials. Vol. 2. Stress intensity factors in bodies with cracks]. Kiyev, Nauk. dumka, 1988. 619 p.
30. Astaf'yev V.I., Radayev Yu.N., Stepanova L.V. *Nelineynaya mekhanika razrusheniya* [Non-linear fracture mechanics]. Samara: Samara University, 2001. 632 p.
31. England A.H. A Crack Between Dissimilar Media. *J. Appl. Mech.*, 1965, vol. 32, pp. 400-402. https://doi.org/10.1115/1.3625813
32. Erdogan F. Stress distribution in bonded dissimilar materials with cracks. *J. Appl. Mech.*, 1965, vol. 32, pp. 403-410. https://doi.org/10.1115/1.3625814
33. Rice J.R., Sih G.C. Plane problems of cracks in dissimilar media. *J. Appl. Mech.*, 1965, vol. 32, pp. 418-423. https://doi.org/10.1115/1.3625816
34. Sih G.C., Chen E.P. *Cracks in composite materials. A compilation of stress solutions for composite systems with cracks*. Springer, 1981. 620 p. https://doi.org/10.1007/978-94-009-8340-3
35. Rice J.R. A path independent integral and the approximate analysis of strain concentration by notches and cracks. *J. Appl. Mech.*, 1968, vol. 35, pp. 379-386. https://doi.org/10.1115/1.3601206
36. Cherepanov G.P. Vychisleniye invariantnykh integralov v osobykh tochkakh [*Computing the invariant integrals in specific locations*] // Vychislitel'nyye metody v mekhanike razrusheniya [Computational methods in the mechanics of fracture], ed. S. Atluri. Moscow, Mir, 1990. Pp. 350-364.
37. Gallo P., Berto F. Some considerations on the J-integral under elastic-plastic conditions for materials obeying a Ramberg–Osgood law. *Phys. Mesomech.*, 2015, vol. 18, pp. 298-306. https://doi.org/10.1134/S1029959915040037
38. Murakami Y. (ed.) *Stress intensity factors handbook*. Pergamon Press, 1987. 1456 p.
39. Astapov N.S., Kornev V.M., Kurguzov V.D. Delamination model for a composite with a crack. *Fiz. mezomekh. – Physical Mesomechanics*, 2016, vol. 19, no. 4, pp. 49-57.
40. Korobeynikov S.N. *Nelineynoye deformirovaniye tverdykh tel* [Nonlinear deformation of solids]. Novosibirsk: Izd-vo SO RAN, 2000. 262 p.
41. MARC 2018. Volume A: Theory and user information. MSC.Software Corporation, 2018. 1008 p.
42. Kurguzov V.D., Kornev V.M., Astapov N.S. Fracture model of bi-material under exfoliation. Numerical experiment. *MKMK – Journal on Composite Mechanics and Design*, 2011, vol. 17, no. 4, pp. 462-473.
43. Kornev V.M., Kurguzov V.D., Astapov N.S. Fracture model of bimaterial under delamination of elasto-plastic structured media. *Appl. Compos. Mater.*, 2013, vol. 20, pp. 129-143. https://doi.org/10.1007/s10443-012-9259-6
44. Kurguzov V.D., Nemirovskiy Yu.V. Modelirovaniye dinamicheskikh protsessov zabivki ili izvlecheniya svay iz grunta [Simulation of dynamic processes of driving or extracting piles from soil]. *Izv. vuzov. Stroitel'stvo – News of higher educational institutions. Construction*, 2011, no. 7, pp. 82-90.
45. Kurguzov V.D., Nemirovsky Yu.V. Mathematical model of dynamic extract of plastic-rigid metal fiber from metal composite. *Izvestiya Altayskogo gosudarstvennogo universiteta – Izvestiya of Altai State University*, 2012, no. 1/1, pp. 69-71.

The authors declare no conflict of interests.
The paper was received on 23.04.2021.
The paper was accepted for publication on 13.08.2021.